

Radiation-Induced Effects on HfO_x-Based Resistive Random Access Memory

K-W Hsu¹, T-H Chang², L. Zhao³, R.J. Agasie⁴, T. B. Betthausen⁵, R.J. Nickles⁵,
Y. Nishi³, Z. Ma², and J.L. Shoet¹

¹Plasma Processing & Technology Laboratory and Department of Electrical & Computer Engineering, University of Wisconsin-Madison, Madison, WI 53706

²Wisconsin Nano Engineering Device Laboratory and Department of Electrical & Computer Engineering, University of Wisconsin-Madison, Madison, WI 53706

³Department of Electrical Engineering, Stanford University, Stanford, CA 94305

⁴Department of Engineering Physics, University of Wisconsin-Madison,
Madison, WI 53706

⁵Waisman Center Brain Imaging PET Laboratory and Department of Medical Physics,
University of Wisconsin-Madison, Madison, WI 53706

ABSTRACT

Neutron and proton induced effects on HfO_x-based Resistive Random Access Memory (RRAM) is investigated. Displacement damage resulting in oxygen vacancies, followed by “annealing” from neutron irradiation and some self-forming of the RRAM cells was observed. An increase in the resistance of the high-resistance state (HRS) of the RRAM may be attributed to the annealing effect. For protons, self-forming was not observed on proton-irradiated RRAM. Thus, there is likely to be less displacement damage during proton irradiation of the same fluence, which is likely caused by coulomb effects. However, a similar increase in the resistance of the HRS as in the case of neutron irradiation was observed. Similarly, protons also annealed the HfO_x film within a RRAM

cell. Shifts in values of the set/reset voltage were observed for both neutron-irradiated and proton-irradiated RRAM cells. We hypothesize that changes to the local atomic structure of HfO_x as a result of neutron and proton irradiation might make defect diffusion difficult.

I. Introduction

Resistive Random Access Memory (RRAM) is considered to be a very promising memory technology and has attracted great attention.¹ As RRAM technology matures and electronic devices using RRAM are likely to be built, malfunctions of RRAM caused by cosmic rays and/or other radiation will become an important problem in industry as the size of these devices continues to decrease.²

In the past, RRAM devices using transition metal oxides, such as TiO_x , HfO_x , and TaO_x have been extensively studied.^{3,4,5} In particular, HfO_x -based RRAM devices show excellent performance in terms of operating current and speed.⁶ Hence, HfO_x -based RRAM devices were chosen as the model system for this work.

About 90% of cosmic rays are protons. The rest of the cosmic-ray composition consists of alpha particles, beta particles, neutrons, heavy ions and some photons (particularly in the x-ray and gamma-ray regions).⁷ Other radiation, such as vacuum ultraviolet (VUV), is often generated during plasma processing.⁸ Among these, protons and neutrons that come from cosmic rays are the most likely ones to cause damage to RRAM based on their fluxes at terrestrial altitudes and their interaction cross sections.⁹

In this work, the primary concern is neutron and proton-induced effects on HfO_x RRAM. The effects on the forming rate, the forming voltage, the resistance of the HRS and the set voltages are investigated.

II. Experimental Configurations

A cross section of an HfO_x RRAM cell used in this work is shown in Fig. 1. The bottom platinum electrode (~90 nm thick) is deposited by e-beam evaporation on a Si wafer with

a two-nm Ti adhesion layer. Then, HfO_x (~25nm) and TiN (~200 nm) layers are deposited by reactive sputtering at room temperature, followed by a lift-off process to generate a pattern on the top electrode.

These RRAM cells were irradiated with neutrons under three different fluences at the University of Wisconsin Max Carbon Radiation-Science Center. The neutron irradiation conditions are shown in Table I. For proton irradiation, 5 MeV and 60 keV protons were generated using both a linear particle accelerator and an ion-implantation facility. Proton irradiation in the MeV range of energies were chosen since cosmic-ray protons are in this range.¹⁰ However, protons lose energy when they pass through matter.¹¹ Thus, lower-energy protons were also investigated. Based on TRIM simulations, 60 keV protons are the most likely to cause damage to the HfO_x film within RRAM. Electrical measurements were made with an HP 4155B semiconductor parameter analyzer. The bottom electrode (Pt) was grounded and the signs of the positive/negative voltages mean positive/negative applied voltage across the cell with respect to the Pt electrode.

Neutron Type	Fluence		
	Thermal ($<1\text{eV}$)	Epithermal ($>1\text{eV}, < 1\text{MeV}$)	Fast ($>1\text{MeV}$)
Low	1.33×10^{12} neutrons/cm ² (X)	3.84×10^{10} neutrons/cm ² (X)	1.76×10^{11} neutrons/cm ² (X)
Medium	10 X	10 X	10 X
High	100X	100X	100 X

III. Results

The investigation of the neutron and proton effects on the HfO_x RRAM cells is separated into two parts. Part A is the effect on the forming process and the resistance of HRS.¹ Part B discusses changes to the set/reset voltages.¹²

According to a review paper published by Wong¹, a forming process is needed for fresh RRAM cells because the number of intrinsic defects in the metal oxide is typically small. To achieve this, a d.c. voltage higher than the set/reset voltage is needed to apply across the oxide. This voltage results in oxygen ions leaving the lattice of the metal oxide and moving toward the anode. This localized deficiency of oxygen leads to the formation of a conduction path¹³ that makes RRAM cells switch to LRS. In subsequent switching cycles, reset or set of the RRAM refers to destruction or reconstruction of the conduction path. However, neutrons and protons could also affect the formation of a conduction path.

I-V characteristics of RRAM cells are also affected by neutron and proton irradiation, especially the resistance of HRS and the set/reset voltage. The increase in the resistance

is related to the changes in defects. The set/reset voltage shifts are considered to be a manifestation of the degradation of the mobility caused by defects.

A. Forming Process and Resistance of HRS

Figure 2 shows the forming rate for RRAM cells irradiated with the three different neutron fluences. Fifty RRAM cells were irradiated with each neutron fluence. The forming rate is the ratio of the number of RRAM cells that were formed and entered the LRS under neutron irradiation to the total number of RRAM cells (which is 50 for each fluence).

The forming rate as a function of neutron fluence is shown in Figure 2. It increases approximately linearly with neutron fluence. Figure 3 shows the forming voltages for unformed RRAM cells that were irradiated with neutrons. The result is shown in Figure 3. From both results, it is apparent that either neutrons alone or a smaller forming voltage after irradiation can result in the formation of the conduction path.

For proton-irradiated RRAM, no RRAM cells were formed even after being exposed to 5 MeV and 60 keV high proton fluence ($\sim 2 \times 10^{15} \text{cm}^{-2}$). The forming voltage for the proton-irradiated RRAM cells is shown in Figure 4. No obvious change in forming voltage after proton irradiation was observed. Thus, for proton-irradiated RRAM cells, no effect is observed in the forming process.

Current of the irradiated RRAM at HRS is always smaller than the pristine RRAM at HRS are shown in Figure 5 and 6. This means that both neutrons and protons “anneal” the RRAM cells by increasing the resistance of the HRS.

The neutron-induced effects on HfO_x RRAM cells agrees with observations from previous work,¹⁴ which showed that neutrons interact with the dielectric material and generate two separate effects: displacement and ionization. In the displacement process, the energy imparted by the incident particles results in atoms leaving their original lattice structure. Once defects are formed by the displacement process, these defects will attempt to reorder to form more stable configurations. Defect reordering results in the annealing process described above. For protons, ionization and displacement processes also occur during irradiation. Thus, less displacement occurs during proton irradiation.

B. Set and reset voltage shifts

Set and reset voltages were also observed for RRAM cells after neutron and proton irradiation shown in the Figure 5 and 6. For pristine RRAM, the set voltage was approximately 3.5 V. The set voltage for neutron-irradiated RRAM increased after irradiation. For proton-irradiated RRAM, the set voltage also increased with either of the two proton energies used here. The increase in set/reset voltages may lead to the hypothesis that changes to the local atomic structure of HfO_x as a result of neutron and proton irradiation might make defect diffusion of difficult.¹⁵ The shifts of the set/reset voltages might lead to a malfunction in RRAM cells because they may no longer be able to switch at fixed applied-pulse voltage. In addition, after an increase in the set voltage in the irradiated RRAM, a much larger power needed for the switching.

IV. Conclusion

Neutron-induced and proton-induced effects on HfO_x RRAM cells were investigated.

Some RRAM cells can be formed by neutron irradiation and appear in the LRS after neutron irradiation. For those unformed irradiated RRAM cells, a smaller forming voltage was needed. In addition, an increase in the HRS resistance was observed in neutron-irradiated RRAM. Furthermore, shifts in values of the set/reset voltage can be seen on the I-V characteristics of neutron-irradiated RRAM cells.

No RRAM cells were formed by proton irradiation after proton irradiation. This was the case even when the energy and fluence of protons were adjusted to increase the interaction between the protons and the dielectric material. In addition, an increase in the HRS resistance was observed in proton-irradiated RRAM. Shifts in values of the set/reset voltage can be seen in the I-V characteristics of proton-irradiated RRAM cells.

V. Acknowledgement

This work was supported by the Semiconductor Research Corporation under Contract No. 2012-KJ-2359, by the National Science Foundation under Grant No. CBET-1066231.

Figure and Table Captions

Table 1. Neutron fluence levels.

FIG.1 Schematic of RRAM cell. HfO_x (~25 nm thick) was deposited with reactive sputtering.

FIG. 2 Forming rate of RRAM cells irradiated with three different neutron fluences.

FIG. 3 Forming voltage of RRAM cells irradiated with three different neutron fluences.

FIG. 4 Forming voltage of RRAM cells irradiated with different proton energies: (a) 5MeV and (b) 60keV. FIG. 5 I-V characteristics of RRAM cells irradiated with three different neutron fluences.

FIG. 6 I-V characteristics of RRAM cells irradiated with different proton energies: (a) 5MeV and (b) 60keV.

References

- ¹H.-S. Philip Wong, H-Y Lee, S. Yu, Y. S. Chen, Y. Wu, P-S Chen, B. Lee, F. T. Chen, and M-J Tsai, "Metal-oxide RRAM," *Proceedings of the IEEE* **100** 1951 (2012).
- ²R. Fang, Y. G. Velo, W. Chen, K. E. Holbert, M. N. Kozicki, H. Barnaby and S. Yu, "Total ionizing dose effect of γ -ray radiation on the switching characteristics and filament stability of HfOx resistive random access memory," *Applied Physics Letters* **104** 183507 (2014).
- ³ S. Kim and Y-K Choi, "A Comprehensive Study of the Resistive Switching Mechanism in-Structured RRAM," *Electron Devices, IEEE Transactions* **56** 3049 (2009).
- ⁴ S. Yu, X. Guan, and H.-S. Philip Wong, "Conduction mechanism of TiN/HfOx/Pt resistive switching memory: A trap-assisted-tunneling model," *Applied Physics Letters* **99** (2011).
- ⁵Z. Wei, Y. Kanzawa, K. Arita, Y. Katoh, K. Kawai, S. Muraoka, S. Mitani, S. Fujii, K. Katayama, M. Iijima, T. Mikawa, T. Ninomiya, R. Miyanaga, Y. Kawashima, K. Tsuji, A. Himeno, T. Okada, R. Azuma, K. Shimakawa, H. Sugaya, and T. Takagi, R. Yasuhara, K. Horiba, H. Kumigashira, and M. Oshima, "Highly reliable TaOx ReRAM and direct evidence of redox reaction mechanism," *IEDM 2008*
- ⁶ H. Y. Lee, P.S. Chen, T.Y. Wu, Y. S. Chen, C. C. Wang, P. J. Tzeng, C.H. Lin, F. Chen, C H. Lien, and M.-J. Tsai, "Low power and high speed bipolar switching with a thin reactive Ti buffer layer in robust HfO2 based RRAM," *IEDM 2008*

⁷ Thomas K. Gaisser, *Cosmic rays and particle physics*, Cambridge University Press, 1-11 (1990)

⁸ H. Ren, G.A. Antonelli, Y. Nishi and J.L. Shohet, "Plasma damage effects on low-k porous organosilicate glass", *Journal of Applied Physics* **108** 094110 (2010).

⁹ E. Petersen, "Soft errors due to protons in the radiation belt," Nuclear Science," IEEE Transactions on **28** 3981 (1981).

¹⁰ J. L. Barth, C. S. Dyer, and E. G. Stassinopoulos, "Space, atmospheric, and terrestrial radiation environments," *IEEE Trans. Nucl. Sci.* **50**, 466 (2003).

¹¹ C. Tschalär, "Straggling distributions of large energy losses," *Nucl. Instrum. Methods* **61**, 141 (1968).

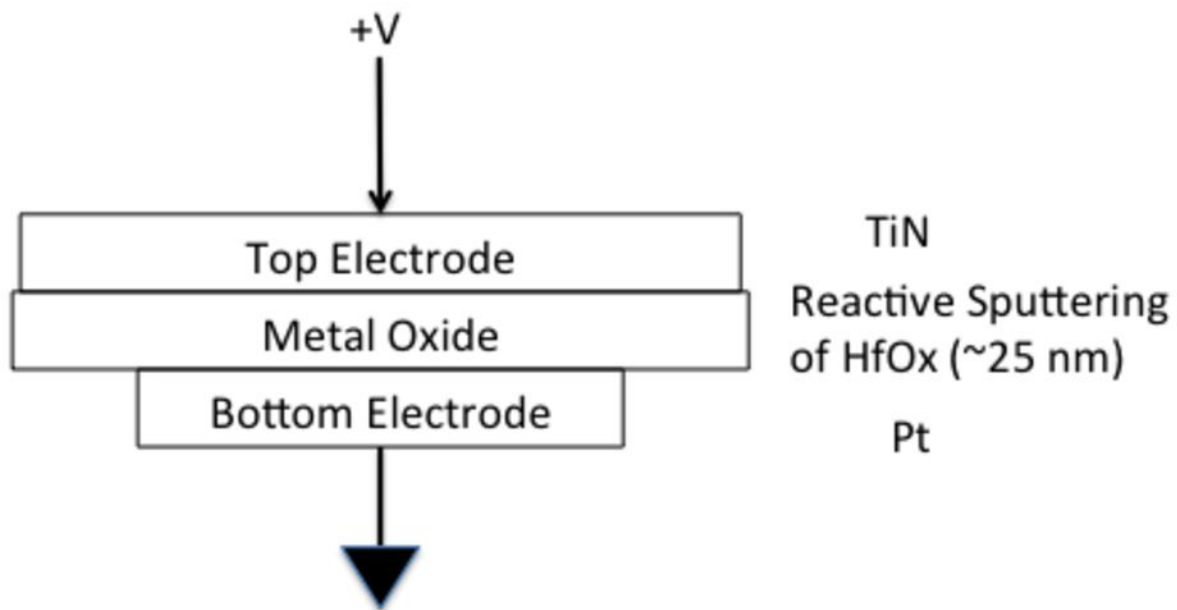
¹² Y. Y. Chen, R. Degraeve, S. Clima, B. Govoreanu, L. Goux, A. Fantini, G. S. Kar, G. Pourtois, G. Groeseneken, D. J. Wouters, "Understanding of the endurance failure in scaled HfO₂-based 1T1R RRAM through vacancy mobility degradation," *Tech. Dig. IEEE Int. Electron Devices Meeting*, 20 (2012).

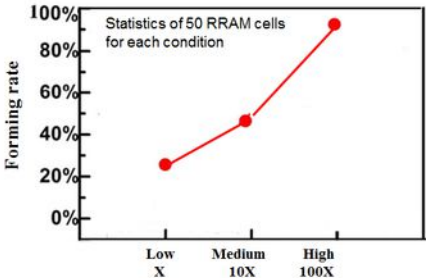
¹³ G. Bersuker, D. C. Gilmer, D. Veksler, P. Kirsch, L. Vandelli, A. Padovani, L. Larcher, K. Mckenna, A. Shluger, V. Iglesias, M. Porti and M. Nafria, "Metal oxide resistive memory switching mechanism based on conductive filament properties," *Journal of Applied Physics* **110** 124518 (2011).

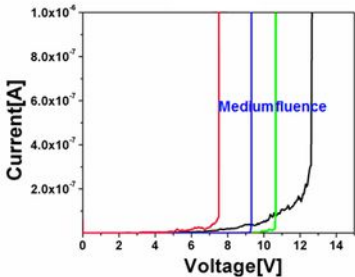
¹⁴ K.-W. Hsu, H. Ren, R. J. Agasie, S. Bian, Y. Nishi and J. L. Shohet, "Effects of neutron irradiation of ultra-thin HfO₂ films," *Applied Physics Letters* **104** 032910 (2014).

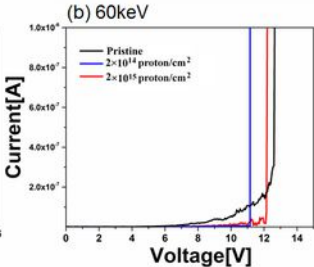
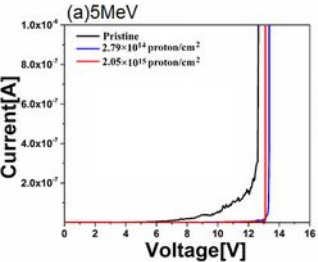
¹⁵ High Neutron Dose Irradiation of Dielectric Mirrors, WWW Document

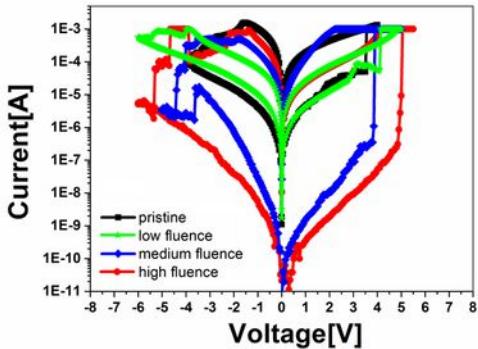
(http://web.ornl.gov/sci/physical_sciences_directorate/mst/fusionreactor/pdf/Vol.55/5.2%20Leonard.pdf)



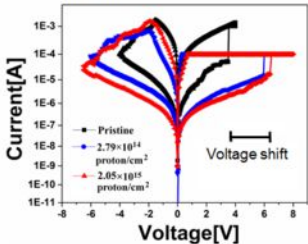








(a) 5MeV



(b) 60keV

